1
Zeolites: A Primer

Pramatha Payra and Prabir K. Dutta
The Ohio State University, Columbus, Ohio, U.S.A.

I. INTRODUCTION TO ZEOLITES

Zeolites are microporous crystalline aluminosilicates, composed of TO_4 tetrahedra (T = Si, Al) with O atoms connecting neighboring tetrahedra. For a completely siliceous structure, combination of TO_4 (T = Si) units in this fashion leads to silica (SiO_2), which is an uncharged solid. Upon incorporation of Al into the silica framework, the +3 charge on the Al makes the framework negatively charged, and requires the presence of extraframework cations (inorganic and organic cations can satisfy this requirement) within the structure to keep the overall framework neutral. The zeolite composition can be best described as having three components:

$$\underset{\text{extraframework cations}}{M^{m+}_{n/m}} \cdot \underset{\text{framework}}{[Si_{1-n}Al_nO_2]} \cdot \underset{\text{sorbed phase}}{nH_2O}$$

The extraframework cations are ion exchangeable and give rise to the rich ion-exchange chemistry of these materials. The novelty of zeolites stems from their microporosity and is a result of the topology of the framework.

The amount of Al within the framework can vary over a wide range, with Si/Al = 1 to ∞, the completely siliceous form being polymorphs of SiO_2. Lowenstein proposed that the lower limit of Si/Al = 1 of a zeolite framework arises because placement of adjacent AlO_4^- tetrahedra is not favored because of electrostatic repulsions between the negative charges. The framework composition depends on the synthesis conditions. Postsynthesis modifications that insert Si or Al into the framework have also been developed. As the Si/Al ratio of the framework increases, the hydrothermal stability as well as the hydrophobicity increases.

Typically, in as-synthesized zeolites, water present during synthesis occupies the internal voids of the zeolite. The sorbed phase and organic non-framework cations can be removed by thermal treatment/oxidation, making the intracrystalline space available. The fact that zeolites retain their structural integrity upon loss of water makes them different from other porous hydrates, such as $CaSO_4$. Figure 1 shows the framework projections and the ring sizes for commonly studied frameworks. The crystalline nature of the framework ensures that the pore openings are uniform throughout the crystal and can readily discriminate against molecules with dimensional differences less than 1 Å, giving rise to the name molecular sieves.

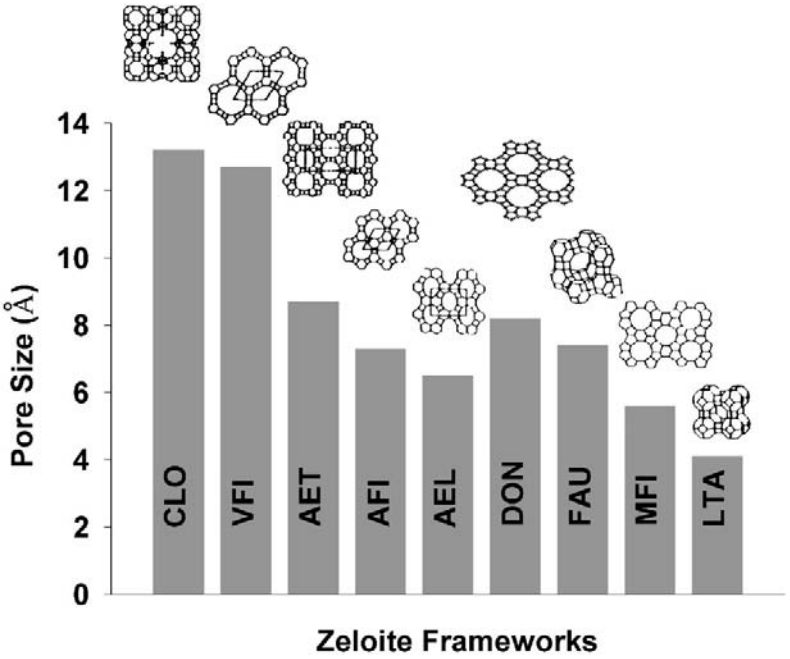

Fig. 1 Comparison of pore sizes of different framework structures.

Though the existence of natural zeolites was noted centuries ago, the field of zeolite science and technology only mushroomed in the 1950s, following the discovery of methods for large-scale industrial synthesis of zeolites by Union Carbide. The inspiration of the industrial work came from the pioneering research by Professor Barrer in zeolite synthesis and adsorption in the mid-1930s and 1940s.

Several textbooks are available on zeolites, including the outstanding monograph by Breck (1–5).

Other elements, such and B, Ge, Zn, P, and transition elements, can also be incorporated into the framework and are referred to as crystalline molecular sieves. Aluminophosphates (AlPOs) have strictly alternating AlO_2^- and PO_2^+ units, and the framework is neutral, organophilic, and nonacidic. The alternation of Al or P leads to structures lacking in odd-numbered rings. Substitution of P by Si leads to silicoaluminophosphates (SAPOs), with cation-exchange abilities. Metal cations can also be introduced into the framework, including transition metal ions such as Co, Fe, Mn, and Zn. Discovery of these solids has led to the development of several new structures (6).

II. ZEOLITE STRUCTURE

The most recent *Atlas of Zeolite Framework Types* lists about 133 framework structures (7). The best criteria for distinguishing zeolites and zeolite-like materials (porous tectosilicates) from denser tectosilicates is the number of tetrahedrally coordinated atoms per 1000 $Å^3$. This number, known as the framework density, is less than 21 T atoms per 1000 $Å^3$ for porous tectosilicates. The angle around the T atoms in the TO_4 tetrahedra are near tetrahedral, whereas the T-O-T bond angles connecting the tetrahedra can vary over a wide range $\sim 125°$ to $\sim 180°$. Liebau and coworkers have proposed a classification for porous tectosilicates that distinguishes between

Table 1 Classification of Porous Tectosilicates

Porosils (SiO_2 based)		Porolites (aluminosilicates)	
Clathrasils	Zeosils	Clathralites	Zeolites
Silica sodalite	Silicalite	Sodalite	Faujasite
	Silica ZSM-22		Mordenite
Dodecasil	SSZ-24		ZSM-5
			Zeolite A

Source: Ref. 8.

aluminous (porolites) and siliceous (porosils) frameworks as well as frameworks that do (zeolites/zeosils) and do not (clathralites/clathrasils) allow exchange of guest species, and is summarized in Table 1 (8). IUPAC recommendations for nomenclature of structural and compositional characteristics of ordered microporous and mesoporous materials with inorganic hosts with particular attention to the chemical composition of both host and guest species, structure of the host, structure of the pore system, and symmetry of the material have been published (9).

The Structure Commission of the International Zeolite Association identifies each framework with a three-letter mnemonic code (7). Table 2 lists the three-letter codes for open four-connected three-dimensional (3D) framework types (7). Thus, the LTA framework encompasses zeolite A, as well as its ion-exchanged forms with K^+ (3A), Na^+ (4A), and Ca^{2+}(5A), frameworks α, ZK-6, N-A, and SAPO-42. Table 3 provides details on some selected zeolite frameworks (10).

Figure 2 shows how the sodalite unit can be assembled to form common zeolitic frameworks: zeolite A (LTA), zeolites X/Y (FAU), and EMT.

Another way to view zeolite structure types involves stacking of units along a particular axis. For example, using the six-ring unit (labeled A), another unit can be vertically stacked over it to generate a hexagonal prism (AA) or offset to generate AB. The third layer can be positioned to form AAA or ABA, AAB or ABB, or ABC. Using such a strategy, Newsom has shown that framework structures of gmelinite, chabazite, offretite, and erionite can be obtained via different stackings of six-membered rings and is shown in Fig. 3 (10). The sequences of erionite (AABAAC) and offretite (AABAAB) show considerable similarity, and is the reason why intergrowths between these two structure types are commonly observed (11).

There are an infinite number of ways of stacking that lead to four-connected three-dimentional (3D) framework structures. Models have been built for large numbers of hypothetical structures (~1000) (12), though only 10% of these frameworks have been observed. The utility of these structural models for aiding in the structure solution of zeolites RHO, EMT, and VPI-5 (VFI) has been documented (13).

III. NATURAL ZEOLITES

Zeolites are found in nature, and the zeolite mineral stilbite was first discovered in 1756 by the Swedish mineralogist A. F. Cronstedt. About 40 natural zeolites are known (14). Most zeolites known to occur in nature are of lower Si/Al ratios, since organic structure–directing agents necessary for formation of siliceous zeolites are absent. Table 2 indicates the natural zeolites. Sometimes natural zeolites are found as large single crystals, though it is very difficult to make large crystals in the laboratory. High-porosity zeolites such as faujasite (FAU), whose laboratory

Table 2 Nomenclature of Zeolites and Molecular Sieves

Si/Al ≤ 2 Low silica	2 < Si/Al ≤ 5 Intermediate silica	5 < Si/Al High silica	Phosphates and other elements
ABW, Li-A(BW)	BHP, linde Q	ASV, ASU-7	ACO, ACP-1
AFG, afghanite[a]	BOG, boggsite[a]	BEA, zeolite β	AEI, $AlPO_4$-18
ANA, analcime[a]	BRE, brewsterite[a]	CFI, CIT-5	AEL, $AlPO_4$-11
BIK, bikitaite[a]	CAS, Cs-aluminosilicate	CON, CIT-1	AEN, AlPO-EN3
CAN, cancrinite[a]	CHA, chabazite[a]	DDR, decadodelcasil 3R	AET, $AlPO_4$-8
EDI, edingtonite[a]	CHI, chiavennite[b]	DOH, dodecasil 1H	AFI, $AlPO_4$-5
FAU, NaX	DAC, dachiardite[a]	DON, UTD-1F	AFN, AlPO-14
FRA, franzinite	EAB, EAB	ESV, ERS-7	AFO, $AlPO_4$-41
GIS, gismondine[a]	EMT, hexagonal faujasite	EUO, EU-1	AFR, SAPO-40
GME, gmelinite[a]	EPI, epistilbite[a]	FER, ferrierite[a]	AFS, MAPSO-46
JBW, NaJ	ERI, erionite[a]	GON, GUS-1	AFT, $AlPO_4$-52
LAU, laumonite[a]	FAU, faujasite[a], NaY	IFR, ITQ-4	AFX, SAPO-56
LEV, levyne[a]	FER, ferrierite[a]	ISV, ITQ-7	AFY, CoAPO-50
LIO, liottite[a]	GOO, goosecreekite[a]	ITE, ITQ-3	AHT, AlPO-H2
LOS, losod	HEU, heulandite[a]	LEV, NU-3	APC, $AlPO_4$-C
LTA, linde Type A	KFI, ZK-5	MEL, ZSM-11	APD, $AlPO_4$-D
LTN, NaZ-21	LOV, lovdarite[b]	MEP, melanopholgite[a]	AST, $AlPO_4$-16
NAT, natrolite[a]	LTA, ZK-4	MFI, ZSM-5	ATF, $AlPO_4$-25
PAR, partheite[a]	LTL, linde L	MFS, ZSM-57	ATN, MAPO-39
PHI, phillipsite[a]	MAZ, mazzite[a]	MSO, MCM-61	ATO, AlPO-31
ROG, roggianite[a]	MEI, ZSM-18	MTF, MCM-35	ATS, MAPO-36
SOD, sodalite	MER, merlinoite[a]	MTN, dodecasil 3C	ATT, $AlPO_4$-12, TAMU
WEN, wenkite[a]	MON, montasommaite[a]	MTT, ZSM-23	ATV, $AlPO_4$-25
THO, thomsonite[a]	MOR, mordenite[a]	MTW, ZSM-12	AWO, AlPO-21
TSC, tschortnerite	OFF, offretite[a]	MWW, MCM-22	AWW, $AlPO_4$-22
	PAU, paulingite[a]	NON, nonasil	BPH, beryllophosphate-H
	RHO, rho	NES, NU-87	CAN, tiptopite[a]
	SOD, sodalite	RSN, RUB-17	CGF, Co-Ga-phosphate-5
	STI, stilbite[a]	RTE, RUB-3	CGS, Co-Ga-phosphate-6
	YUG, yugawaralite[a]	RTH, RUB-13	CHA, SAPO-47
		RUT, RUB-10	CLO, cloverite
		SFE, SSZ-48	CZP, chiral zincophosphate
		SFF, SSZ-44	ERI, $AlPO_4$-17
		SGT, sigma-2	DFO, DAF-1
		SOD, sodalite	DFT, DAF-2
		STF, SSZ-35	FAU, SAPO-37
		STT, SSZ-23	GIS, $MgAPO_4$-43
		TER, terranovaite	OSI, UiO-6
		TON, theta-1	RHO, pahasapaite[a]
		ZSM-48	SAO, STA-1
		VET, VPI-8	SAS, STA-6
		VNI, VPI-9	SAT, STA-2
		VSV, VPI-7	SAV, Mg-STA-7
			SBE, UCSB-8Co
			SBS, UCSB-6GaCo
			SOD, $AlPO_4$-20
			SBT, UCSB-10GaZn
			VFI, VPI-5
			WEI, weinebeneite
			ZON, ZAPO-M1

[a] Natural materials.
[b] Beryllosilicates (natural).
Source: Ref. 7.

analogs are zeolites X/Y, are scarce. This is not surprising considering their metastable structures and conversion to more condensed forms. Also, high-porosity zeolites are formed in the laboratory under narrow synthesis compositions. Two natural zeolites that find extensive use are clinoptilolite (HEU) and mordenite (MOR) for ion-exchange (radioactive) agricultural uses and as sorbents. The catalytic activity of natural zeolites is limited by their impurities and low surface areas. Another natural zeolite, erionite (ERI), has toxicity comparable to or even worse than some of the most potent forms of asbestos, especially in causing a form of lung mesothelioma (15).

IV. ZEOLITE SYNTHESIS

The evolution of materials development in the zeolite field over the last 50 years has followed a path of steady progress, along with steady leaps that introduce new paradigms of synthesis. Flanigen, one of the pioneers in this field, has summarized the development as shown in Table 4 (16).

A. Low-Silica or Al-Rich Zeolites

Milton and Breck at Union Carbide reported the discovery of zeolites A and X in 1959. Even though many new frameworks have been discovered since then, these zeolites still enjoy tremendous academic and commercial importance. Zeolites A and X have the highest cation contents and are excellent ion-exchange agents.

B. Intermediate Silica Zeolites

Breck reported the synthesis of zeolite Y in 1964, which spans a Si/Al ratio of 1.5–3.8 and with framework topology similar to that of zeolite X and the mineral faujasite. Decreasing the Al content led to both thermal and acid stabilities and paved the way for development of zeolite Y–based processes in hydrocarbon transformations. Large–port mordenite, also with a Si/Al ratio of 5, was reported by Sand (17).

C. High-Silica Zeolites

Zeolites with Si/Al ratios of 10–100 (or higher) were reported by Mobil Research and Development Laboratories in the 1960s and 1970s, with the best known example being ZSM-5 (18,19). Even though the Al content is low, the acidity manifested by these zeolites is adequate for hydrocarbon catalysis reactions.

The early zeolite syntheses involved hydrothermal crystallization of reactive alkali-based aluminosilicates at low temperatures (<100°C), resulting in low Si/Al ratio materials, and the role of the alkali cations as structure-directing agents was proposed (1,2). Addition of organic species to aluminosilicate and silicate gels led to synthesis of high-silica zeolites and all-silica molecular sieves. The temperatures of these syntheses are often above 100°C and the organic reagent can act as a void filler, charge balancer, structure-directing agent, and, in some cases, a true template (20). Typical examples of cation directing agents for ZSM-5 are shown in Table 5 (21). The International Zeolite Association recently put together a monograph on synthesis of zeolitic materials, where each synthesis has been verified independently (22).

Postsynthesis enrichment of silicon in the framework have been reported by several procedures, including hydrothermal steaming, as well as use of aqueous $(NH_4)_2SiF_6$ and $SiCl_4$ and F_2 gases (23). Postsynthesis modifications of zeolites are technologically important, as in production of siliceous zeolite Y by removal of framework aluminum for catalytic cracking

Table 3 Characteristics of Selected Zeolite Frameworks

Code	Examples[a]	Typical Si(T-Si) ratio	Occ[b]	Maximal[c] space group	SBU[d]	FD[e]	N_T[f]	Pore structure[g]
ABW	Li-A(BW), $Cs[SiAlO_4]$	1.0	S	I*mam*	4, 6, 8	19.0	8	**8** 3.4 × 3.8*
AFI	AlO_4-5	1.0	S	P6/*mcc*	4, 6	17.5	24	**12** 7.3*
AFS	MAPSO-46	1.0	S	$P6_3/mcm$	61	13.7	56	**12** 6.3* ↔ 8 4.0 × 4.0**
ANA	Analcime, leicite, pollucite, viseite, wairakite, Na-B $AlPO_4$-24, $Cs_2[FeSi_5O_{12}]$	2.0	NS	I*a3d*	4, 6, 6-2	18.6	48	**8** distorted
BEA	Beta,[h] NU-2[h]	10.0	S	$P4_122$	5-1 + 4	15.5	64	**12** 7.3 × 6.0**
CAN	Cancrinite, tiptopite, ECR-5	1.0	NS	$P6_3/mmc$	6	16.7	12	**12** 5.9*
CHA	Chabazite, linde D, linde R, ZK-14, SAPO-34, MeAPO-47	2.0	S	R3*m*	6, 6-6	14.6	36	**8** 3.8 × 3.8*
EDI	Edingtonite, K-F, linde F	1.5	NS	$P42_1m$	4=1	16.6	10	**8** 2.8 × 3.8* ↔ 8 variable
EMT	ZSM-20[i]	4.5	S	$P6_3/mmc$	6-6, 6-2	12.7	192	**12** 7.6 ↔ **12** 7.6 × 5.7***
ERI	Erionite, linde T[j], AlO_4-17	3.0	NS	$P6_3/mmc$	6	15.6	36	**8** 3.6 × 5.1***
FAU	Faujasite, linde X, linde Y, LZ-210, SAPO-37	2.5	NS	Fd3*m*	6-6, 6-2	12.7	192	**12** 7.4***
FER	Ferrierite, Sr-D, FU-9, ZSM-35, ISI-6	5.0	NS	I*mmm*	5-1	17.7	36	**10** 4.2 × 5.4* ↔ **8** 3.5 × 4.8*
HEU	Heulandite, clinoptilolite, LZ-219	3.5	NS	C2/*m*	4-4=1	17.0	36	**8** 2.6 × 4.7* ↔ {**10** 3.0 × 7.6* + **8** 3.3 × 4.6*
KFI	ZK-5, Ba-P, Ba-Q	2.0	S	I*m3m*	6-6, 4, 8, 6-2	14.7	96	**8** 3.9***|3.9***
LTA	Linde A, ZK-4, N-A, alpha, ZK-21, ZK-22, SAPO-42	1.0	S	P*m3m*	4-4, 8, 6-2	12.9	24	**8** 4.1***

LTL	Linde L, K(Ba)G(L), ECR-3, perlialite	3.0	NS	P6/*mmm*	6	16.4	36	**12** 7.1*
MAZ	Mazzite, omega, ZSM-4	3.0	NS	$P6_3/mmc$	5-1, 4	16.1	36	**12** 7.4* ↔ 8 3.4 × 5.6*
MEL	ZSM-11	>30.0	S	I4*m*2	5-1	17.7	96	**12** 5.3 × 5.4***
MFI	ZSM-5, silicate AMS-1B, NU-4	>15.0	S	P*nma*	5-1	17.9	96	**10** 5.3 × 5.6* ↔ {**10** 5.1 × 5.5}***
MOR	Mordenite, ptilolite, Zeolon, Na-D	5.0	NS	C*mcm*	5-1	17.2	48	**12** 6.7 × 7.0* ↔ **8** 2.6 × 5.7*
MTN	ZSM-39, Dodecasil 3C	α	S	F*d*3*m*	5+5-1	18.7	136	**6**
MTW	ZSM-12, CZH-5, NU-13	>40.0	S	C2/*m*	5-1+4	19.4	28	**12** 5.5 × 5.9*
NAT	Natrolite, mesolite, scolecite	1.5	NS	$I4_1/amd$	4=1	17.8	40	**8** 2.6 × 3.9* ↔ **8** variable*
OFF	Offretite, TMA-O, linde T[j]	3.5	NS	P6*m*2	6	15.5	18	**12** 6.7* ↔ **8** 3.6 × 4.9**
RHO	Rho, pahasapaite	3.0	NS	I*m*3*m*	8-8, 6, 6-2	14.3	48	**8** 3.6***|3.6***
SOD	Sodalite, ultramarine, nosean, tugtupite, $AlPO_4$-20	1.0	NS	I*m*3*m*	6, 4, 6-2	17.2	12	**6**
TON	Theta-1, Nu-10, KZ-2, ISI-1, ZSM-22	>30.0	S	C*mcm*	6, 5-1	19.7	24	**10** 4.4 × 5.5*
VFI	VPI-5, $AlPO_4$, $AlPO_4$-54, MCM-9	1.0	S	$P6_3/mcm$	4-2	14.2	36	**18** 11.2*

[a] Type species on which framework code is based is given first.
[b] Occurrence: N, natural mineral; S, synthetic; NS, both.
[c] Highest symmetry for the framework type; symmetries actually adopted by example materials may be lower.
[d] Secondary building unit. Frequently more than one is appropriate, and only the most useful are given.
[e] Framework density in T atoms per 1000 $Å^3$.
[f] Number of T atoms in the (highest symmetry) unit cell.
[g] Nomenclature of Meier and Olson. Bold numbers indicate number of T (or O) atoms in the defining ring. Approximate aperture free diameters are then given for the type species in Å, the number of asterisks indicating if the channel system is one-, two-, or three-dimensional. For more than one channel↔ (or |) indicates whether (or not) channels interconnect.
[h] Structure comprises *bea-beb* intergrowths.
[i] Structure comprises FAU-EMT intergrowths.
[j] Structure comprises ERI-OFF intergrowths.
Source: Ref. 10.

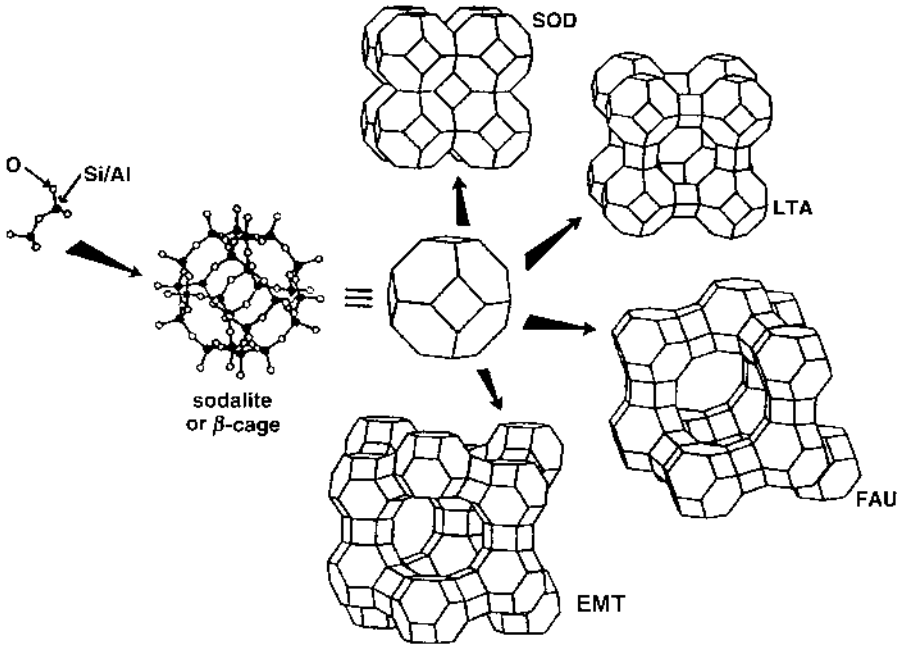

Fig. 2 The construction of four different zeolite frameworks with sodalite or β cages. A pair of TO_4 tetrahedra is linked to a single sodalite cage by T-O-T bonds. In a less cluttered representation, the oxygen atoms are omitted and straight lines are drawn connecting the tetrahedral (T) atoms. The sodalite cage unit is found in SOD, LTA, and FAU,-EMT frameworks. (From Ref. 10.)

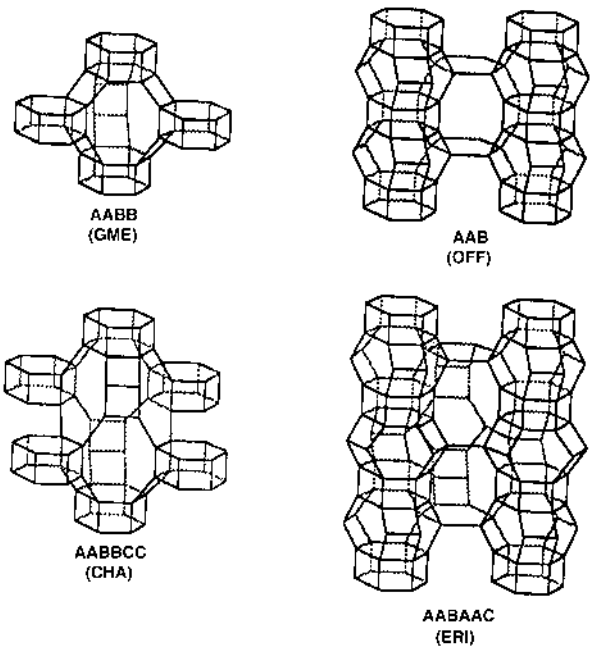

Fig. 3 Schematic illustration how different modes of stacking of six-ring units in superposition or offset give rise to a series of structure types, including gmelinite (GME), chabazite (CHA), offretite (OFF), and erionite (ERI). (From Ref. 10.)

Table 4 The Evolution of Molecular Sieve Materials

"Low" Si/Al zeolites (1–1.5)	A, X
"Intermediate" Si/Al zeolites (~2–5)	A) Natural zeolites: erionite, chabazite, clinoptilolite, mordenite
	B) Synthetic zeolites: Y, L, large-pore mordenite, omega
"High" Si/Al zeolites (~10–100)	A) By thermochemical framework modification: highly silicious variants of Y, mordenite, erionite
	B) By direct synthesis: ZSM-5, Silicate
Silica molecular sieves	

Source: Ref. 16.

applications. Dealumination results in frameworks with greater thermal stability and enhanced catalytic properties (24). Aluminum, though displaced from the framework, as evident by unit cell contraction, can still be present in the zeolite and modify its catalytic properties. In all cases, microporosity arises from amorphous regions of the modified zeolite, with the extent depending upon the process, the most severe being steaming.

V. ZEOLITE CHARACTERIZATION

X-ray powder diffraction is the most common method for determining the zeolite structure as well as its purity (25). In that regard, the book *Collection of Simulated XRD Powder Patterns of Zeolites* is most valuable and also provides information about the space group and unit cell parameters (26).

Scanning electron microscopy (SEM) is the method of choice for determining the size and morphology of zeolite crystallites. High-resolution transmission electron microscopy has been extensively used to study intergrowth fault planes and stacking faults and recently for structural analysis (27).

Common spectroscopic methods for analyzing zeolite structure include magic angle spinning ^{29}Si and ^{27}Al nuclear magnetic resonance (NMR) spectroscopy (28–30). Information regarding the coordination environment around Si and Al and the framework Si/Al ratio can be obtained. Infrared spectroscopy via the frequencies of structure-sensitive bands provides information regarding framework properties, including Si/Al ratios and nature of acidity by

Table 5 Organic Molecules Used for Synthesis of ZSM-5

Tetrapropylammonium	Di-*n*-propylamine
Tetraethylammonium	1,5-Diaminopentane
Tripropylamine	1,6-Diaminohexane
Ethyldiamine	Morpholine
Propanolamine	Pentaerythritol
Ethanolamine	Dipropylenetriamine
Methyl quinuclide	Dihexamethylenetriamine
NH_3 + alcohol	Triethylenetetramine
Alcohols	Diethylenetetramine
Glycerol	1-alkyl-4-azonibicyclo[2,2,2]octane-4-oxide halide
n-Propylamine	Hexanediol
Di-*n*-butylamine	Propylamine

Source: Ref. 21.

the -OH stretching vibration (31,32). Other techniques used include Raman spectroscopy, which provides information complementary to infrared, electron paramagnetic resonance for analyzing the coordination environment of nonframework and framework metal ions, X-ray fluorescence spectroscopy for elemental analysis, and X-ray photoelectron spectroscopy for surface analysis (33–37).

Synchrotron-based diffraction experiments are also finding considerable use for structural analysis (38). In addition, computational chemistry is now aiding structure analysis, modeling of synthetic pathways, and chemical reactivity (39).

VI. ZEOLITE POROSITY

Access to the intracrystalline void of zeolites occurs through rings composed of T and O atoms. For rings that contain 6 T atoms (six-membered rings or 6 MR) or less, the size of the window is ~2 Å, and movement of species through these rings is restricted. Ions or molecules can be trapped in cages bound by rings of this size or smaller (5 MR, 4 MR, 3 MR). For zeolites containing larger rings, ions and molecules can enter the intracrystalline space. Figure 4 shows the primary pore system of some common zeolites (10).

The internal volume of zeolites consists of interconnected cages or channels, which can have dimensionalities of one to three. Pore sizes can vary from 0.2 to 0.8 nm, and pore volumes from 0.10 to 0.35 cm^3/g. The framework can exhibit some flexibility with changes in temperature and via guest molecule–host interaction, as noted for the orthorhombic-monoclinic transformations in ZSM-5 (40).

Most detailed information about the pore structure comes from the crystal structure analysis. Adsorption measurements also provide data on the pore system, based on the minimal size of molecules that can be excluded from the interior of the zeolite (41,42). ^{129}Xe NMR spectroscopy, via the chemical shifts of ^{129}Xe, provides information about the porosity in zeolites, especially those that have been modified, e.g., by coke formation during cracking (43,44).

Figure 5 demonstrates that in the range of porosity typically found in zeolites, the intracrystalline diffusivities can change by 12 orders of magnitude depending on the pore size and the size and shape of the molecule diffusing through the zeolite (45).

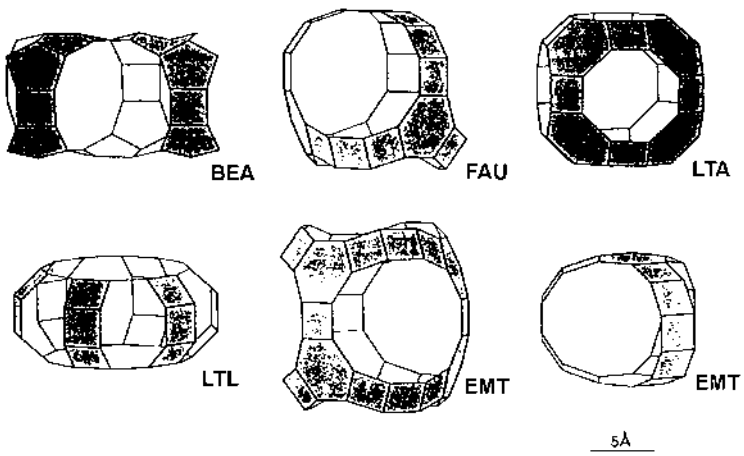

Fig. 4 Representation of the primary pore systems of several important zeolites, T-O-T bonds are drawn as straight lines. Data are taken from representative crystal structures and drawn to the same scale. (From Ref. 10.)

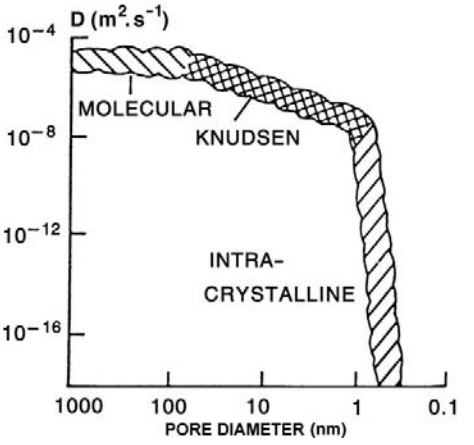

Fig. 5 Effect of pore diameter on molecular diffusivity, showing that intrazeolitic diffusion can span more than 10 orders of magnitude. (From Ref. 45.)

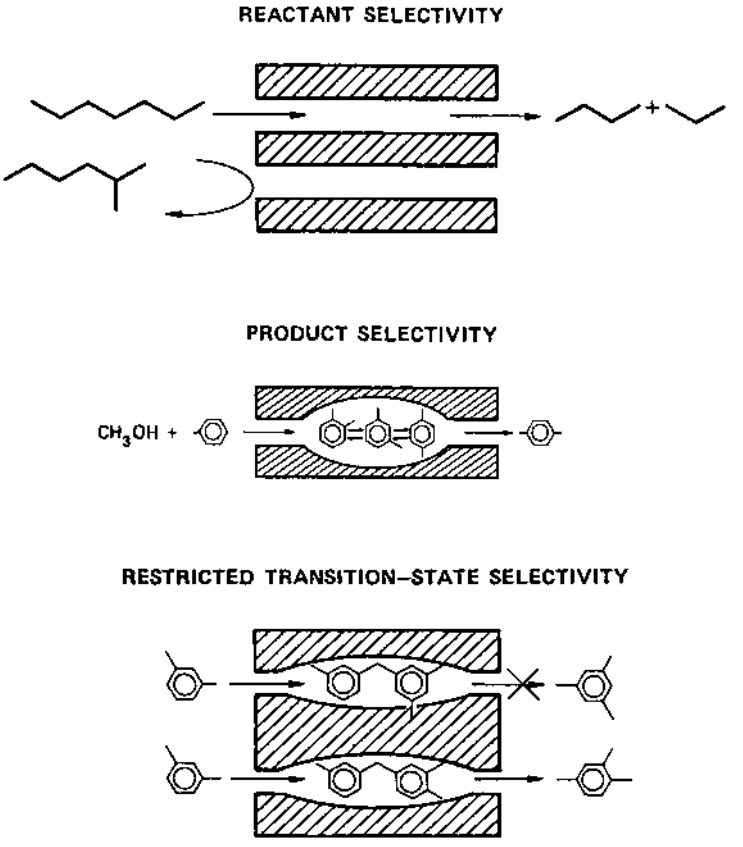

Fig. 6 Different types of reaction selectivity imposed by the rigid pore structure of the zeolite. (From. Ref. 46.)

The rigid pore structure leads to steric constraints on molecules within the zeolite resulting in novel reaction pathways in comparison with unconstrained media. This is demonstrated in Fig. 6 as examples of reactant, product, and transition state selectivities (46). The increase in size upon methyl substitution is enough to prevent the alkane from entering the zeolite. The higher diffusivity of *p*-xylene by a few orders of magnitude in the channel system of the zeolite in comparison with the o and m isomers facilitates selectivity toward the product. Another example is that of molecular traffic control in ZSM-5, where reactant molecules diffuse through one channel system, while product molecules diffuse through the other channel, minimizing counterdiffusion (47).

Several model compound–based cracking reactions have been developed to provide information about the pore system (48). One of these is the constraint index (CI), which compares the rate constants for cracking of 1:1 mixtures of *n*-hexane and 3-methylpentane. The pore classification involves CI < 1 for large pores, 1 < CI < 12 for intermediate pores, and CI > 12 for small pores. This index takes advantage of the fact that the methyl branch in 3-methylpentane excludes the molecule from small-pore zeolites.

The pore opening can also be controlled via ion exchange. For Na-A (LTA), the ~4 Å opening allows removal of CO_2 from CH_4. For K-A with a ~3 Å opening, H_2O can be removed from alcohols and alkanes. For Ca-A with ~4.7 Å opening, *n*-alkanes can penetrate the zeolite, but branched alkanes are excluded (49). Important information about pore dimensions and framework structures is found in *Atlas of Zeolite Structure Types* (6).

VII. ZEOLITE PROPERTIES

Thermal stability of zeolites varies over a large temperature range. The decomposition temperature for Low-silica zeolites is ~700°C, whereas completely siliceous zeolite, such as silicalite, is stable up to 1300°C. Low-silica zeolites are unstable in acid, whereas high-silica zeolites are stable in boiling mineral acids, though unstable in basic solution. Low-silica zeolites tend to have structures with 4, 6, and 8 MR, whereas more siliceous zeolites contain 5 MR. Low-silica zeolites are hydrophilic, whereas high-silica zeolites are hydrophobic and the transition occurs around Si/Al ratios of ~10.

Cation concentration, siting, and exchange selectivity vary significantly with Si/Al ratios and play an important role in adsorption, catalysis, and ion-exchange applications. Though acid site concentration decreases with increase in Si/Al ratio, the acid strength and proton activity coefficients increase with decreasing aluminum content. Zeolites are also characterized by the unique property that the internal surface is highly accessible and can compose more than 98% of the total surface area. Surface areas are typically of the order of 300–700 m^2/g.

Zeolite acidity is important for hydrocarbon transformation reactions (48,50). Both Bronsted and Lewis acid sites are found and several methods have been developed to determine acidity. Chemical method includes temperature-programmed desorption (TPD), which exploits the fact that more thermal energy is required to detach a base from stronger acid sites than weaker acidic sites. Typical bases used are NH_3 or pyridine. This method cannot distinguish between Bronsted or Lewis sites. In order to do so, infrared spectroscopy is the method of choice. For example, pyridine can be adsorbed as pyridinium ion on a Bronsted site whereas it is coordinatively bonded to a Lewis acid site. The vibrational frequencies are distinct, with the Lewis-bound site appearing at 1450 and 1600 cm^{-1}, and the Bronsted-bound site at 1520 and 1620 cm^{-1}.

Both thermodynamic and kinetic aspects of ion-exchange processes in zeolites are active areas of research (51,52). Ion-exchange isotherms provide a measure of the selectivity of one ion over another. Isotherms also provide information regarding phase transformations during

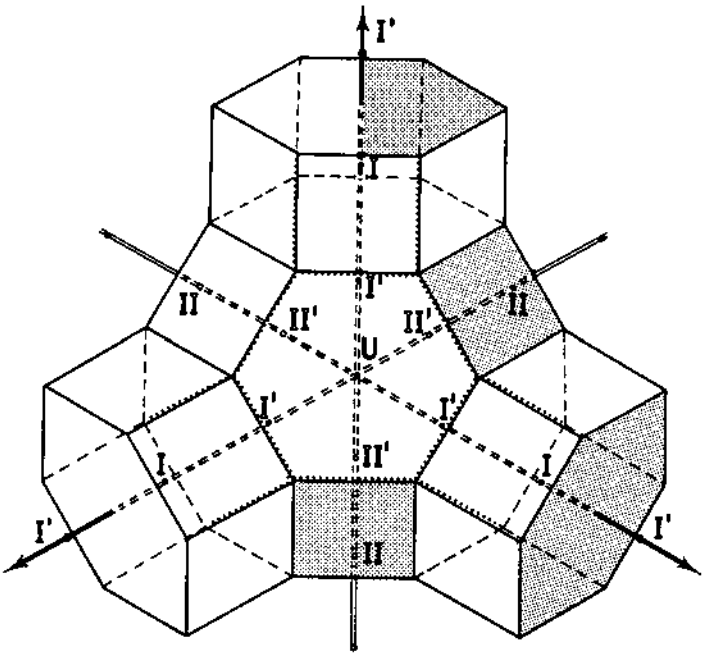

Fig. 7 The cation sites in the faujasite framework. Site I is in the hexagonal prism (D6R); I′ is near the entrance to a hexagonal prism in the sodalite (β) cage. II′ is inside the sodalite cage near the single-6R entrances to the large (α) cage. II is in the large cage adjacent to D6R and U is at the center of the sodalite cage. Other sites (IV, V) are in the large supercage cavities. (From Ref. 53.)

exchange or if exchange is limited because of exclusion of a cation. In some cases, a cation cannot access parts of the crystal due to its large size (ion sieving), or the cation takes up too much intrazeolitic volume (volume exclusion) thereby excluding other ions. In a particular zeolite, there can be several sites, as shown in Fig. 7 for zeolite Y (53). These sites have specific energies and characteristic cation populations. Ion-exchange kinetics, though of considerable importance in zeolite applications such as catalysis and in detergent action, has not been as extensively studied because of the complexity of the process. Diffusion of ions can be rate limiting within the crystal (particle-controlled diffusion) or in passing through the zeolite-fluid boundary (surface diffusion), with the latter becoming more important for smaller crystallite size. Within the crystal, diffusion is promoted by concentration gradients as well as influenced by electrical potential gradients due to the charge density differences of the exchanging ions. Because of non-steady-state ion transport, present models are quite inadequate to describe the experimental results.

VIII. ZEOLITE MODELING

Computational chemistry is playing an increasingly important role in all aspects of zeolite science (39,54–56). In the area of zeolite synthesis, the study of possible synthesis intermediates, as well as organic–inorganic interactions, is an active area of research. Structural calculations have focused on lattice stability, cation positions, and lattice vibrational modes. The basic research have focused on development of appropriate potentials. Quantum mechanical calculations on small clusters have been used to probe Bronsted acidity, as well as binding of small organic molecules and subsequent protonation (57,58). Computer simulations have played a major part in analyzing adsorption by Monte Carlo methods and molecular transport by

molecular dynamics techniques (59,60). Calculation of adsorption enthalpies and diffusivity in zeolites for organic species is now possible.

IX. APPLICATIONS OF ZEOLITES

Zeolites are extensively used in primarily three applications: adsorbents, catalysts, ion exchange. In addition, natural zeolites because of their lower cost are used in bulk mineral applications.

A. Adsorbent Applications

Table 6 lists the common adsorbent applications and focuses on removal of small polar or polarizable molecules by more aluminous zeolites and bulk separations based on molecular sieving processes (61,62).

B. Catalyst Applications

Table 7 lists the principal applications of catalysis by zeolites. Hydrocarbon transformation of zeolites is promoted by the strong acidity of zeolites prepared via certain pathways, including NH_4^+ and multivalent cation exchange, and via steaming. Besides acidity, the other unique feature of zeolite relates to a concentration effect of reactants within the cages/channels and promotes bimolecular reactions, such as efficient intermolecular hydrogen transfer. For more siliceous zeolites, the organophilic nature promotes the conversion of polar oxygenated hydrocarbons to paraffins and aromatics. Zeolites are also finding increasing use for synthesis of organic intermediates and fine chemicals. Advantages of zeolites that are being exploited include heterogenization of catalysts for easy separation framework, doping with metals for selective oxidation chemistry, and ease of regeneration of catalysts (63–69).

In Table 8 is correlated the discovery of new frameworks with the number of U.S. patents and their commercial importance (70). The table shows that even though there has been an accelerated discovery of new frameworks and patents for their composition and use over the last 50 years, only a very small fraction ever find application in commercial processes.

Table 6 Commercial Adsorbent Applications of Molecular Sieve Zeolites

A. Purification	B. Bulk separations
Drying:	Normal/iso-paraffin separation
natural gas (including LNG)	
cracking gas (ethylene plants)	Xylene separation
insulated windows	
refrigerant	
CO_2 removal:	Olefin separation
natural gas, flue gas ($CO_2 + N_2$)	Separation of organic solvents
cryogenic air separation plants	
Sulfur compound removal	O_2 from air
Sweetening of natural gas and liquified petroleum gas	Separation of CO_2, SO_2, NH_3
Pollution abatement: removal of Hg, NO_x, SO_x	Sugar separation
Removal of organic and inorganic iodide compounds from commercial acetic acid feed streams	Separation of amino acids, *n*-nitrosoamines

Source: Ref. 16.

Table 7 Applications of Zeolites in Catalysis

Inorganic reactions:	Hydrocarbon conversion:
H_2S oxidation	Alkylation
NO reduction of NH_3	Cracking
CO oxidation, reduction	Hydrocracking
CO_2 hydrogenation	Isomerization
$H_2O \rightarrow O_2 + H_2$	
Organic reactions:	
Aromatization (C_4 hydrocarbons)	Dehydration
Aromatics (disproportionation, hydroalkylation, hydrogenation, hydroxylation, nitration, oxidation, oxyhalogenation, hydrodecyclization, etc.)	Epoxidation (cyclohexene, olefins, α-pinene, propylene, styrene)
Aldol condensation	Friedel-Craft reaction of aromatic compounds (alkylation of butylphenol with cinnamyl alcohol)
Alkylation (aniline, benzene, biphenyl, ethylbenzene, naphthalene, polyaromatics, etc.)	Fischer-Tropsh reaction (CO hydrogenation)
Beckman rearrangement (cyclohexanone to caprolactam)	Methanol to gasoline
Chiral (enantioselective) hydrogenation	Methanation
CH_4 (activation, photocatalytic oxidation)	MPV (Meerwin-Ponndorf-Verley) reduction (transfer hydrogenation of unsaturated ketones)
Chloroaromatics dechlorination	Oxyhalogenation of aromatics
Chlorination of diphenylmethane	Heck reaction (acetophenone + acrylate → acrylate ester)
Chlorocarbon oxidation	Hydrogenation and dehydrogenation
Chlorofluorocarbon decomposition	Hydrodealkylation
Cinnamaldehyde hydrogenation	Shape-selective reforming
Cinnamate ester synthesis	
Cyclohexane (aromatization, isomerization, oxidation, ring opening)	

Source: Refs. 16 and 73.

Table 8 Zeolite Discovery and Use by Decade

Decade	Known structure types	U.S. patents, composition or use	Commercialized structure types
1950–1969	27	2,900	3
1970–1979	11	4,900	1
1980–1989	26	7,400	2
1990–1999	61	8,200	5
Totals	125	23,400	11

Source: Ref. 70.

Table 9 Ion Exchange Applications and Advantages

Applications	Advantage
Removal of Cs^+ and Sr^{2+}	Stable to ionizing radiation
Radioisotopes—LINDE AW-500, Mordenite, clinoptilolite	Low solubility, dimensional stability, High selectivity
Removal of NH_4^+ from wastewater—LINDE F, LINDE W, clinoptilolite	NH_4^+-selective over competing cations
Detergent builder zeolite A, zeolite X (ZB-100, ZB-300)	Remove Ca^{2+} and Mg^{2+} by selective exchange, no environmental problem
Radioactive waste storage	Same as Cs^+, Sr^+ removal
Aquaculture(AW-500, clinoptilolite)	NH_4^+ selective
Regeneration of artificial kidney dialysate solution	NH_4^+ selective
Feeding NPN to ruminant animals	Reduces NH_4^+ by selective exchange to nontoxic levels
Metals removal and recovery	High selectivities for various metals
Ion exchange fertilizers	Exchange with plant nutrients such as NH_4^+ and K^+ with slow release in soil

Source: Ref. 16.

Table 10 Summary of Uses of Natural Zeolites

Bulk applications:	Molecular sieve applications:
Filler in paper	• Separation of oxygen and nitrogen from air
Pozzoolanic cements and concrete	
Dimension stone	• Acid-resistant adsorbents in drying and purification
Lightweight aggregate	
Fertilizers and soil conditioners	• Ion exchangers in pollution abatement processes
Dietary supplement in animal nutrition	

Source: Ref. 16.

Table 11 Health Science and Zeolites

Detoxification of mycotoxins by selective binding with zeolites	Biomedical applications:
Insects control: semiochemicals adsorbed in zeolites and by controlling diffusion-deisorption rate controls concentration of the pheromones in the air.	External application Detoxicants Decontaminants Vaccine adjuvants
Reaction of clinoptilolite and human bile	Antibacterial agents
Protein (cytochrome *c*) adsorption. Encapsulation and immobilization of proteinaceous materials in zeolite.	Enzyme mimetics Drug delivery Diabetes mellitus
Poultry industry: feed additive, toxin binder for environmental protection and for converting hen manure to deodorized fertilizer	Antitumor adjuvants Antidiarrheal agents Hemodialysis
Milk yield, consumption, carcass characteristics in lactating cows	Contrast in magnetic resonance
Diets of farm animals: gain, feed conversion, dressing percentage, carcass characteristics of lambs	Bone formation Biosensors

Source: Ref. 73.

C. Ion-Exchange Applications

Table 9 lists ion-exchange applications of zeolites (71,72). The major use of zeolites as ion-exchange agents is for water softening applications in the detergent industry and substitute use of phosphates. The selectivity of zeolite A for Ca^{2+} provides a unique advantage. Natural zeolites find considerable use for removal of Cs^{+} and Sr^{2+} radioisotopes by ion exchange from radioactive waste streams, as listed in Table 10.

D. Other Applications

Table 11 provides examples of health-related applications of zeolites. These were compiled from the proceedings of the recent international zeolite conference (73). Zeolitic membranes offer the possibility of organic transformations and separations coupled into one unit. Redox molecular sieves are expected to find use in synthesis of fine chemicals, exploiting both the considerable flexibility in designing the framework topology and insertion of reactive elements and compounds into the framework, as exemplified in Table 7. Other niche applications include sensors, photochemical organic transformations, and conversion of solar energy (74–77). Bulk applications for zeolite powders have emerged for odor removal and as plastic additives.

REFERENCES

1. DW Breck. Zeolite Molecular Sieves. New York: Wiley, 1974.
2. RM Barrer. Hydrothermal Chemistry of Zeolites. London: Academic Press, 1982.
3. A Dyer. An Introduction to Zeolite Molecular Sieves. New York: Wiley, 1988.
4. S Bhatia. Zeolite Catalysis: Principles and Applications. Boca Raton: CRC Press, 1990.
5. R Szostak, Handbook of Molecular Sieves. New York: Van Nostrand Reinhold, 1992.
6. CK Cheetham, G Ferey, T Loiseau. Angew Chem Int Ed 38:3268–3292, 1999.
7. Ch Baerlocher, WM Meier, D Holson. Atlas of Zeolite Framework Types. Amsterdam: Elsevier, 2001.
8. F Liebau, H Gies, RP Gunawardne, B Marles. Zeolites 6:373–377, 1986.
9. LB McCusker, F. Liebau, G. Engelhardt. Pure Appl Chem 73:381–394, 2001.
10. JM Newsam. In: AK Cheetham, P Day, eds. Solid State Chemistry: Compounds. New York: Oxford University Press, 1992, pp. 234–280.
11. A Gualtieri, G Artioli, E Passaglia, S Bigi, A Viani, JC Hanson. Am Mineral 83:590–606, 1998.
12. MD Foster, RG Bell, J Klinowski. In: A Galarneau, F Di Renzo, F Fajula, J Vedrine, eds. Zeolites and mesoporous materials at the dawn of the 21st century. Stud Surf Sci Catal 135:2747–2754, 2001.
13. LB McCusker, C Baerlocher, E Jahn, M Buelow. Zeolites 11:308–313, 1991.
14. RW Tschernich. Zeolites of the World. Phoenix: Geoscience Press, 1992.
15. GD Guthrie. Environ Health Persp 105:1003–1011, 1997
16. EM Flanigen. Pure Appl Chem 52:2191–2211, 1980.
17. WL Kranich, YH Ma, LB Sand, AH Weiss, I Zwiebel. Adv Chem Ser 101:502–513, 1971.
18. RJ Argauer, GR Landolt. US Patent 3702886 (1972).
19. DH Olson, GT Kokotaillo, SL Lawton, WM Meier. J Phys Chem 85:2238–2243, 1981.
20. MM Helmkamp, ME Davis. Annu Rev Mater Sci 25:161–192, 1995.
21. BM Lok, TR Cannan, CA Messina. Zeolites 3:282–291, 1983.
22. H Robson. Verified Syntheses of Zeolitic Materials. Amsterdam: Elsevier, 2001.
23. R Szostak. In: H van Bekkum, EM Flanigen, JC Jansen, eds. Introduction to Zeolite Science and Practice. Stud Surf Sci Catal 58:153–199, 1991.
24. RA Beyerlein, GB McVicker. In: ML Occelli, ed. Fluid Catalytic Cracking V: Materials and Technological Innovations. Stud Surf Sci Catal 134:3–40, 2001.

25. GT Kokotailo, CA, Fyfe, Y Feng, H Grondey, H Gies, B Marler. Stud Surf Sci Catal 94:78–100, 1995.
26. MM J Treacy, JB Higgins, R von Ballmoos. Zeolites 16:327–802, 1996.
27. JM Thomas, O Terasaki, PL Gai, W Zhou, J Gonzales-Calbet. Acc Chem Res 34:583–594, 2001.
28. HG Karge, M Hunger, HK Beyer. Characterization of zeolites-infrared and nuclear magnetic resonance spectroscopy and x-ray diffraction. In: J Weitkamp, L Puppe, eds. Catalysis and Zeolites: Fundamentals and Applications. Berlin: Springer-Verlag, 1999, 198–326.
29. DF Shantz, RF Lobo. Top Catal 9:1–11, 1999.
30. CA Fyfe, Y Feng, H Grondey, GT Kokotailo, H Gies. Chem Rev 91:1525–1543, 1991.
31. C Arean. Inorg Chem 22:241–273, 2000.
32. HG Karge. Micropor Mesopor Mater 22:547–549, 1998.
33. P-P Knops-Gerrits, DE De Vos, EJP Feijen, PA Jacobs. Micropor Mater 9:3–17, 1997.
34. N Ortins, T Kruger, PK Dutta. In: M Pelletier, ed. Analytical Application of Raman Spectroscopy. Oxford: Blackwell, 1999, pp. 328–366.
35. D Biglino, H Li, R Erckson, A Lund, H Yahiro, M Shiotani. Phys Chem Chem Phys 1:2887–2896, 1999.
36. M Stocker. Micropor Mater 6:235–257, 1996.
37. AE Pillay, M Peisach. J Radioanal Nucl Chem 153:75–84, 1991.
38. K Knorr, F Madler, RJ Papoular. Microporous Mesopor Mater 12:353–363, 1998.
39. CRA Catlow. Modeling of Structure and Reactivity in Zeolites. London: Academic Press, 1992.
40. H van Koningsveld, JC Jansen, H van Bekkum. Zeolites 10:235–2472, 1990.
41. J. Karger, DM Ruthven, eds. Diffusion in Zeolites and other Microporous Solids. New York: John Wiley, 1992.
42. EG Derouane. J Mol Catal A: Chem 134:29–45, 1998.
43. JA Ripmeester, CI Ratcliffe. J Phys Chem 94:7652–7656, 1990.
44. JL Bonardet, MC Barrage, J Fraissard, MA Ferrero, WC Conner. Stud Surf Sci Catal 88:265–271, 1994.
45. MFM Post. In: H Van Bekkum, EM Flamigen, JC Jansen, eds. Introduction to Zeolite Science and Practice. Stud Surf Sci Catal 58:391–444, 1991.
46. SM Csicsery. Zeolites 4:202–213, 1984.
47. EG Derouane, Z Gabelica. J Catal 65:486–489, 1980.
48. PA Jacobs. Carboniogenic Activity of Zeolites. Amsterdam: Elsevier, 1977.
49. G Guan, K Kusakabe, S Morooka. Sep Sci Technol 36:2233–2245, 2001.
50. E Brunner, H Pfeifer. Anal Meth Instrum 2:315–329, 1995.
51. AM Tolmachev, EM Kuznetsova. Spec Publ R Soc Chem 182:274–281, 1996.
52. A Dyer. Inorg Ion Exch Chem Anal:33–55, 1991.
53. JV Smith. In: EM Flanigen, LB Sand, eds. Molecular Sieve Zeolites-I. ACS Symposium Series 101:173, 1971.
54. B Van de Graaf, SL Njo, KS Smirnov. Rev Comput Chem 14:137–223, 2000.
55. FJ Keil, R Krishna, M-O Coppens. Rev Chem Eng 16:71–197, 2000.
56. GM Zhidomirov, AL Yakovlev, MA Milov, HN Kachurovskaya, IV Yudanov. Catal Today 51: 397–410, 1999.
57. MV Frash, RA Van Santen. Top Catal 9:191–205, 1999.
58. D Nicholson, R J-M Pellenq. Adv Colloid Interf Sci 76–77:179–202, 1998.
59. SM Auerbach. Int Rev Phys Chem 19:155–198, 2000.
60. DM Ruthven. Chem Eng Prog 84:42–50, 1988.
61. F Fajula, D Plee. In: JC Jansen, M Stöcker, HG Karge, J Weitkamp, eds. Advanced Zeolite Science and Applications. Stud Surf Sci Catal 85:633–651, 1994.
62. D Barthomeuf. Catal Rev Sci Eng 38:521–612, 1996.
63. G Ertl, H Knozinger, J Weitkamp. Preparation of Solid Catalysts. Weinheim: Wiley-VCH, 1999.
64. JM Garces, A Kuperman, DM Millar, MM Olken, AJ Pyzik, W Rafaniello. Adv Mater 12:1725–1735, 2000.
65. PB Weisz. Micropor Mesopor Mater 35–36:1–9, 2000.

66. SJ Kulkarni. In: TSR Prasada Rao, G Murali Dhar, eds. Recent Advances in Basic and Applied Aspects of Industrial Catalysis. Stud Surf Sci Catal 113:151–161, 1998.
67. Y Izumi. Zeolite, Clay and Heteropoly Acid in Organic Reactions. New York: VCH, 1992.
68. DE De Vos, BF Sels, PA Jacobs. Adv Catal 46:1–87, 2001.
69. TF Degnan, Jr. Top Catal 13:349–356, 2000.
70. MW Schoonover, MJ Cohn. Top Catal 13:367–372, 2000.
71. GH Kuhl. In: J Weitkamp, L Puppe, eds. Catal Zeolites. Berlin: Spinger-Verlag, 1999, 81–197.
72. P Misaelides, F Macasek, TJ Pinnavaia, C Coletta, eds. Natural Microporous Materials in Environmental Technology. Dordrecht: Kluwer Academic, 1999.
73. A Galarneau, F Di Renzo, F Fajula, J Vedrine, eds. Zeolites and Mesoporous Materials at the Dawn of the 21st Century. Stud Surf Sci Catal 135:2001.
74. S Mintova, T Bein. Micropor Mesopor Mater 50:159–166, 2001.
75. V Ramamurthy. J Photochem Photobiol C 1:145–166, 2000.
76. KB Yoon. Mol. Supramol Photochem 5:143–251, 2000.
77. AS Vaidyalingam, MA Coutant, PK Dutta. In: V. Balzani, ed. Electron Transfer in Chemistry, Vol. 4. New York: Wiley-VCH, 2001, pp. 412–486.